

Article citation info:

Wang F, Doszhan R, Wang S, Xu F, He J, Wang M, Zheng L, Optimizing Integrated Energy Systems with Hierarchical Dual-Level Algorithms in the Electrical Internet of Things Framework for Improved Renewable Energy Utilization and Cost Efficiency, *Eksploatacja i Niezawodność – Maintenance and Reliability* 2025; 27(4) <http://doi.org/10.17531/ein/206051>

Optimizing Integrated Energy Systems with Hierarchical Dual-Level Algorithms in the Electrical Internet of Things Framework for Improved Renewable Energy Utilization and Cost Efficiency

Indexed by:



Fushuai Wang ^a, Raigul Doszhan ^{a, *}, Shichao Wang ^a, Fumin Xu ^b, Junda He ^c, Mengxia Wang ^c, Liwei Zheng ^d

^a Farabi Business School, Al-Farabi Kazakh National University, Kazakhstan

^b Shandong Tourism Development Research Center, Shandong College of Tourism and Hospitality, China

^c Zhejiang University of Technology, China

^d Beijing Talent Technology Co, China

Highlights

- A Bayesian-based reliability analysis method by fusing prior and test data is proposed.
- The prior data are expanded using neural network in combination with simulation data.
- The mechanism kinematic accuracy reliability is quantified under small-sample condition.
- The key variables affecting the retraction mechanism reliability are identified.

Abstract

This study proposes a novel integrated system (IES) model to promote load distribution and thermal energy management by considering the turbulence effects, dynamic pressure fluctuations, and the nonlinear efficiency of energy conversion processes. This framework enhances the mass and energy balance equations, thus enhancing the accuracy of the hydraulic and thermal loss estimates. Further, a demand response (DR) model is also created, accounting for stochastic fluctuations in thermal and electrical demands and incorporating cross-elasticity effects. This will enable a more accurate representation of the consumer's reactions to changes in the pricing. We employ a modified particle swarm optimization (MPSO) algorithm to optimize the energy dispatch strategy. The modified version includes adjustable learning rates and changing inertia weights, which help it find solutions faster and more accurately. The algorithm successfully manages the distribution of electricity and heat energy, taking into account how energy storage works and the complexities in the conversion systems.

Keywords

electrical Internet of things, modified PSO, integrated energy systems, energy dispatch optimization, combined heat and power, demand response.

This is an open access article under the CC BY license (<https://creativecommons.org/licenses/by/4.0/>)

1. Introduction

1.1. Background and motivation

The increasing integration of renewable energy sources into modern power systems has introduced significant operational and economic challenges, necessitating advanced optimization

strategies for efficient energy management [1]. Traditional energy supply systems, relying on centralized control systems, are challenged to cope with the intermittent nature of renewable energy production and customer consumption [2]. IESs offer

(*) Corresponding author.
E-mail addresses:

F. Wang (ORCID: 0000-0001-7659-8107) fushuaiwang1993@gmail.com, R. Doszhan (ORCID: 0009-0008-6447-9459) raiguldoszhan1993@gmail.com, S. Wang (ORCID: 0009-0008-8718-1225) shichaowang1993@gmail.com, F. Xu (ORCID: 0009-0004-4329-4982) fuminxu1994@gmail.com, J. He (ORCID: 0009-0004-3019-3146) vincent@zjut.edu.cn, M. Wang (ORCID: 0009-0003-0727-2658) mengxiawang1993@gmail.com, L. Zheng (ORCID: 0009-0009-9059-5936) liweizheng93@gmail.com

a feasible solution through various combinations of energy carriers, including electricity and thermal energy, to improve system optimization and flexibility. The development of energy management policies has also been affected by the advent of electrical Internet of Things (EIoT), which includes features consisting of real-time monitoring, smart scheduling of load, and predictive maintenance techniques [3]. By leveraging smart sensors with improved sensing technologies, data analysis, and enabling adaptive controls, EIoT ensures enhanced efficiency and reliability in integrated energy networks [4]. The intricate management of diverse energy sources and uncertainty in renewable energy production and utilization calls for high-level computing methods for optimizing system performance. The use of hierarchical dual-level optimization is one promising technique for IES dispatch to address such challenges. The technique allows for integrated decision-making at all levels of the energy system, thus promoting better economic optimization along with simultaneous operational flexibility [5]. Nevertheless, even with their potentials, such optimization techniques often do not effectively embrace IES's nonlinear behavior as well as relationships that limit their applicability. The present work introduces a novel optimization framework that integrates an MPSO technique in hierarchical dispatch to enhance the use of renewable energy sources along with cost-effectiveness.

1.2. Literature review

Much research work has gone into investigating various optimization methods and models to improve the efficiency of IESs. This section provides a comprehensive review of the research conducted on optimization methods and models for IESs. Kong et al. [6] optimized IES using the Power Internet of Things (PIoT) framework. Enhanced information exchange in IES ensures greater network flexibility in interactions. The work introduces a new DR model that uses a two-level economic dispatch system to enhance overall performance and better manage resources on the demand side. The focus is on improving system performance and optimizing demand-side resource allocation. Ye et al. [7] highlighted that the overuse of traditional energy sources drives the need for carbon emission reduction to combat global warming. IESs enhance renewable energy use and efficiency, but uncertainties in generation and

demand complicate optimization. To address this, power-to-gas technology is integrated for electricity-heat-gas cogeneration and CO₂ absorption, with a carbon emission factor included to assess both economic and environmental impacts. Dou et al. [8] highlighted that the rise of renewable energy makes renewable-based heat-electricity IESs a viable solution. The dispatch and scheduling of renewable-based heat-electricity IESs is complex due to economic, environmental, and security factors. In the study, a multi-objective hierarchical deep reinforcement learning method is proposed, using a multi-critic, single-actor structure to optimize objectives with decoupled rewards and hierarchical action value functions. Lei et al. [9] proposed a market-based model for decentralized operation in multi-microgrid systems to improve power distribution efficiency and reliability. Microgrids, consisting of controllable and uncontrollable generation units, storage systems, and loads, exchange energy within a network. Using IoT technology and cloud infrastructure, the system enables efficient data measurement, processing, and the exchange of technical and financial information. Jiang et al. [10] expressed that energy transformation and consumption improvements have advanced the planning and use of diverse energy sources. With the growth of IESs, integrated DR can help by reducing demand and facilitating the conversion and storage of energy, allowing users to engage more in network regulation. They introduced the concept of integrated DR, its hierarchical structure, and adaptable response resources, categorizing integrated DR into four response modes based on load management and user involvement. Zhou and Liu [11] highlighted that the rapid growth of digital technologies is driving the energy revolution, but their roles in sustainable transitions remain unclear. Their study reviewed advancements in these technologies for energy efficiency and integration, focusing on their impact on high-efficiency, low-carbon building systems, including AI for performance predictions and optimization of systems like PVs, heat pumps, and multi-energy storage. Wu et al. [12] explored electricity trading in a deregulated retail market, aiming to coordinate energy consumption through DR and carbon emission mechanisms under dynamic pricing. Their goal was to minimize IES operating costs while balancing supply and demand. The challenge arises from the competitive interaction among prosumers, modeled as a Stackelberg-Nash game with

the retailer as the leader and PV prosumers as followers. Bahmanyar et al. [13] studied targeted research in IoT-based home energy management systems for the smart grid's demand side, with the ability to provide an advanced appliance scheduling, which would shift consumption from peak to off-peak intervals. The multi-objective Archimedes Optimization algorithm with inclusions of Raspberry Pi, Node-RED, and NodeMCU modules was proposed for minimizing electricity costs and peak-to-average ratio while enhancing UC under the real-time-price and critical peak pricing tariff structures. Kazemi et al. [14] proposed an IoT-enabled approach to reduce costs and improve reliability in multi-carrier energy hubs (EHs) and IESs with renewable resources, CHP, and plug-in hybrid electric vehicles. The model used price-based DR to manage electrical and thermal demands in multi-EHs. By shifting loads during peak hours, energy bills were reduced, and renewable energy uncertainties were addressed. Simulation results highlighted the model's effectiveness in optimizing power and heat exchange, demonstrating its potential for cost-effective and reliable energy management in micro EHs. Masoomi et al. [15] studied the digitization of Renewable energy systems, focusing on the integration of clean energy and its optimization. The research identified barriers to IoT adoption in emerging economies like India, categorizing 16 issues into five dimensions. Technology barriers were found to be the primary challenge. Recommendations included structural and technological improvements, proactive governance, and updated market frameworks to enhance IoT integration with renewable energy for a smoother energy transition. Gao et al. [16] highlighted that buildings account for 40 % of primary energy use and 36 % of greenhouse gas emissions. They developed a new IoT-based framework for zero-energy building energy modeling to address variable loads, occupant comfort, and thermal issues. The system optimized heating, ventilation, and air conditioning control using deep reinforcement learning and aligned energy usage with solar production. It managed building loads, electric vehicle charging, and energy storage, with empirical validation showing its potential for sustainable zero-energy buildings. Kumar et al. [17] explored the transformative impact of Industry 4.0 technologies on IoT in warehousing and logistics. The study revealed that IoT research was more focused on logistics than warehousing, with most

studies from industrialized countries and limited theoretical frameworks. Lv et al. [18] analyzed the challenges and opportunities of Industrial IoT and digital twin for monitoring hazardous gas leakage. They proposed an optimization framework, using a three-tier edge computing network and a dual-stage tracking algorithm, efficiently tracked gas boundaries, reduced energy consumption, and showed high accuracy. Humayun et al. [19] proposed an energy optimization methodology for smart cities, leveraging IoT, 5G networks, and cloud computing to reduce energy consumption in areas like street lighting, billboard ads, smart homes, and intelligent parking. IoT sensors detected motion, 5G enabled low-latency data transfer, and cloud computing supported storage and processing, offering significant potential for improving energy efficiency in urban settings. Kuthadi et al. [20] addressed data dissemination issues in IoT-based wireless sensor networks, proposing an optimized energy management model for data dissemination. This framework, using non-adaptive routing, collaborative systems, and priority planning, increased data transmission by 96.33 % and reduced energy consumption by 20.11 %, demonstrating its effectiveness. Kolhe et al. [21] highlighted the importance of technology in addressing urbanization challenges and enhancing resilience in smart cities, especially during disasters. This study used IoT with cloud computing to collect and normalize data, applying the Advanced Random Forest algorithm for machine-to-machine interaction. The proposed adaptive cloud computing virtual machine resource allocation technique optimization method showed improved efficiency in simulations, supporting smart city development. Rind et al. [22] explored the evolution of smart energy systems, highlighting their integration across sectors like power, smart grids, and logistics through communication technologies and cloud computing. They emphasized advancements in sensing, communication, and system integration, which have enhanced the precision, reliability, and adaptability of smart energy systems. Smart meters were also discussed as key IoT devices, becoming more complex and adaptable for flexible designs. Saleem et al. [23] presented a smart energy management system utilizing IoT technology to optimize energy usage, emphasizing demand-side management to improve efficiency and decrease costs. The system linked devices to energy controllers equipped with sensors and

actuators, aggregated data for real-time analysis through a centralized cloud middleware, and underwent testing in four buildings. Jia et al. [24] discussed how IoT revolutionized renewable energy integration by improving efficiency, reliability, and sustainability in power systems. IoT enables real-time monitoring, data analysis, and automation for load management, DR, and energy storage. Despite challenges like data security and communication standardization, key developments such as smart grids and energy management systems have enhanced grid stability. The study also highlighted IoT's role in electric vehicle performance through improved battery management.

Majhi et al. [25] explored how IoT is transforming power systems for sustainable, low-carbon energy solutions. They identified IoT applications including renewable energy integration, automation of power plants, smart protection devices, smart homes, and smart meters. While IoT shows significant potential for the power sector, challenges remain, and the review provided insights for decision-making and further development in this field. Bai et al. [26] developed a framework for energy consumption and decarbonization optimization in Industrial IoT, considering IESs, carbon capture, hydrogen storage, and carbon trading. Using CPLEX, they optimized energy procurement, carbon trading costs, and carbon dioxide sales, showing significant reductions in operational costs and carbon footprints. Sharma et al. [27] proposed an AI-based framework for optimal electricity demand load shifting, reducing power outages and peak-to-average ratio in grid loads. By utilizing IoT devices and machine learning algorithms, the framework analyzed real-time and historical data to forecast and shift energy demands, improving load optimization, distribution efficiency, and offering cost-saving opportunities for utilities and consumers.

1.3. The previous scientific gaps and research gaps

In recent years, significant advancements have been made in the optimization of IESs, particularly in the context of enhancing renewable energy utilization and improving cost efficiency. However, several gaps persist in the existing research, particularly regarding the efficient coordination of multi-energy systems under fluctuating renewable generation and demand patterns. Traditional optimization methods often fail to account

for the nonlinearities inherent in energy conversion processes and the complex interdependencies between various energy carriers. Moreover, many existing frameworks lack the ability to adapt to the dynamic nature of energy systems, particularly in integrating real-time data from smart sensors and IoT-enabled devices. Additionally, while DR models have been integrated into IES frameworks, they often oversimplify consumer behavior or fail to capture the full spectrum of stochastic variations in energy consumption. Modern models presented in the literature have problems with effectively integrating various energy sources, such as electricity, heat, and gas, mainly due to their inability to optimize energy distribution in thermal and electrical sectors. In addition, traditional optimization methods, for instance, traditional particle swarm optimization (PSO), typically have slow rates of convergence along with being suboptimal in solving complicated, multi-objective problems associated with IES.

This study remedies these deficiencies through the presentation of a new optimization technique comprising an MPSO algorithm within a bi-level dispatching system. It improves the accuracy and efficiency of electric and thermal energy distribution through consideration of the dynamic and complex natures of energy conversion systems. The MPSO algorithm enhances the solution quality and speed of discovery by employing variable learning rates and adaptive inertia weights, thereby addressing the slow convergence and precision issues of conventional PSO. Moreover, this study proposes a DR model that captures the behavior of customers as a reaction to the random variations in electricity and heating demand, as well as their reaction to price changes. The two-level optimization model enables us to include various sources of energy, which makes the IES more flexible and responsive, and hence more appropriate for real-world applications where renewable energy generation and consumption may have large variations. The key contributions and novelties presented in this paper are as follows:

1. Presenting a novel dual-level dispatch strategy for IESs, optimizing both electrical and thermal energy dispatch simultaneously.
2. Employing an MPSO algorithm to solve the optimization problem. The MPSO algorithm is designed to enhance the speed of convergence and

solution accuracy compared to traditional optimization methods, making it highly effective for complex, nonlinear, multi-objective problems in IES.

3. Introducing a more advanced DR model, which captures the stochastic variations in electrical and thermal loads. This model accounts for real-time pricing fluctuations and better reflects consumer behavior, filling a critical gap in traditional DR strategies.
4. Integrating diverse energy sources, including electricity, heat, and gas, into a unified optimization framework. It enables the dynamic and efficient management of energy resources, enhancing the overall performance and sustainability of the IES.
5. Enhancing applicability to real-world energy systems by adapting to fluctuating renewable energy generation and demand variations defines the strength of the optimization framework.

2. Problem formulation

2.1. Electrical Internet of Things

The EIoT, situated across four distinct layers - perception, network, platform, and application - represents a transformative paradigm for enhancing energy systems. Each layer is crucial for the functionality and efficacy of the system, as it facilitates advanced monitoring, data collection, and analysis that enhance decision-making inside IESs [6]. Important parts include data collection, edge computing, and other edge infrastructures working together at the comprehension layer to provide thorough information gathering and effective monitoring of appliances. Depending on the application, communication channels between edge computer systems and sensing devices vary using technologies like Ethernet, PLC, RS-485, or another suitable approach. Supporting perfect connection with 4G, 5G, and fiber optic technologies, the system layer facilitates data flow between the demand side and the transmission core. Analyzing the data acquired from the edge computing system, the platform layer maintains open channels of communication to the dispersion center and conducts analysis. At last, the operations center controls the system's functioning coordination while the application layer shows the user interface utilizing mobile applications or other devices, therefore allowing the user

to engage with the IES.

The integration of EIoT into energy systems, particularly in the dispatching and management of resources, presents both opportunities and challenges. An IES, as a multifaceted framework that includes energy routers and devices for conversion, storage, and connection of diverse energy sources, has the potential to address the dynamic needs of various sectors such as education, production, and residential life. The rise of EIoT has revolutionized the distribution system of IESs by expanding the scope of load-side data collection. This data now includes electrical and thermal energy consumption, along with parameters such as voltage, frequency, mass flow rate, and temperature. In addition, the frequency of these checks has increased from daily to hourly or even every 15 minutes, creating a huge amount of data volume. Augmentations in data flow bring increases in decision-making platforms' accuracy and efficiency, but they raise daunting challenges in terms of data transmission, processing speed, and costs in the dispatch center. The effectiveness of a cloud-edge scheduling system in tackling these challenges comes from edge computing, which does some calculations before sending combined data to dispatch center for scheduling. This minimizes communication bottlenecks, reduces processing speed, and ensures user privacy. The graded dispatching method, influenced by EIoT, allows for energy system distribution through a structured approach, where edge computing resources manage the lower levels of distribution and energy support. The dispatch center optimally manages controllable facilities, including electric generators, thermal generators, CHP systems, and renewable production, while controlling load-side control to enhance energy efficiency and minimize operational expenses. This approach not only optimizes energy resource distribution but also ensures a more responsive and efficient energy system that meets the demands of modern communities.

2.2. Integrated load distribution

Expanding the hydraulic model to include turbulence effects and dynamic pressure corrections, the mass flow balance is now given by [28]:

$$m^q(i, t) = \sum_{l \in L^{in,S}(i,t)} \left(m^S(l, t) - \alpha K^S(l, t) m^S(l, t)^2 - \frac{\delta P(l, t)}{R^S(l)} \right) - \sum_{l \in L^{out,S}(i,t)} m^S(l, t) \quad (1)$$

$$m^q(i, t) = \sum_{l \in L^{in,R}(i,t)} \left(m^R(l, t) - \beta K^R(l, t) m^R(l, t)^2 - \frac{\delta P(l, t)}{R^R(l)} \right) - \sum_{l \in L^{out,R}(i,t)} m^R(l, t) \quad (2)$$

Additionally, pressure drop equations incorporating Darcy-Weisbach friction loss and minor losses are given as:

$$\delta P(l, t) = \frac{f(l)L^{Pipe}(l)}{D(l)} \frac{\rho}{2} m^2(l, t) + \sum_j \xi_j \frac{\rho}{2} m^2(l, t) \quad (3)$$

To improve thermal loss estimation, heat transport is modeled dynamically:

$$T^{out,S}(l, t) = T^{Am}(t) + \left(T^{in,S}(l, t) - T^{Solid}(l, t) \right) \cdot \exp\left(\frac{\lambda(l)L^{Pipe}(l)}{Cm^S(l, t) + \gamma T^{out,S}(l, t)} \right) \quad (4)$$

$$T^{out,R}(l, t) = T^{Am}(t) + \left(T^{in,R}(l, t) - T^{Solid}(l, t) \right) \cdot \exp\left(\frac{\lambda(l)L^{Pipe}(l)}{Cm^R(l, t) + \gamma T^{out,R}(l, t)} \right) \quad (5)$$

$$Q_{loss}(l, t) = \lambda(l)L^{Pipe}(l) \left(T^{avg}(l, t) - T^{Am}(t) \right) \quad (6)$$

The temperature of a node considering thermal mixing is:

$$T^S(i, t) = \frac{\sum_{l \in L^{in,S}(i,t)} m^S(l, t) T^{out,S}(l, t)}{\sum_{l \in L^{in,S}(i,t)} m^S(l, t)} \quad (7)$$

$$T^R(i, t) = \frac{\sum_{l \in L^{in,R}(i,t)} m^R(l, t) T^{out,R}(l, t)}{\sum_{l \in L^{in,R}(i,t)} m^R(l, t)} \quad (8)$$

The load DR to pricing and stochastic variations is:

$$D_H(i, t) = D_H^{base}(i) \left(1 - \eta_H \frac{P_H(t) - P_H^{ref}}{P_H^{ref}} + \xi_H \mathcal{N}(0, \sigma_H^2) \right) \quad (9)$$

$$D_E(i, t) = D_E^{base}(i) \left(1 - \eta_E \frac{P_E(t) - P_E^{ref}}{P_E^{ref}} + \xi_E \mathcal{N}(0, \sigma_E^2) \right) \quad (10)$$

The total energy balance at a node account for electric and thermal storage systems:

$$E_{storage}(t+1) = E_{storage}(t) + \eta_{ch} P_{ch}(t) - \frac{P_{dis}(t)}{\eta_{dis}} \quad (11)$$

$$Q_{storage}(t+1) = Q_{storage}(t) + \eta_{ch} Q_{ch}(t) - \frac{Q_{dis}(t)}{\eta_{dis}} \quad (12)$$

The iterative solution for balancing mass and thermal equations is:

$$X^{(k+1)} = X^{(k)} - J^{-1}(\Delta F + \phi \nabla \Delta F) \quad (13)$$

2.3. Load estimation and load response program

The heat load estimation model is refined by incorporating thermal inertia effects, dynamic heat transfer coefficients, and internal heat generation (e.g., occupants, appliances) [29]. The temperature evolution equation is given by:

$$T^{Bui}(i, t + \Delta t) = T^{Bui}(i, t) e^{\left(-\frac{\Delta t}{\tau^{Bui}(i,t)} \right)} + \left(1 - e^{\left(-\frac{\Delta t}{\tau^{Bui}(i,t)} \right)} \right) \cdot \left(T^{Am}(t) + \frac{H^{Load}(i, t) + H^{Int}(i, t)}{R^{Air}(i, t)} \right) \quad (14)$$

The thermal demand elasticity is now modeled as a nonlinear function of price variations to better capture real-world consumer behavior:

$$E^H(i, t) = \frac{\Delta H^{Load}(i, t)}{\rho^{(DR,H)}(t)} \cdot \frac{\rho^H(t)}{H^{(Load,Ori)}(i, t)} + \xi_H \mathcal{N}(0, \sigma_H^2) \quad (15)$$

$$H^{Load}(i, t) = H^{(Load,Ori)}(i, t) \cdot \left[1 + E^H(i, t) \cdot \left(\frac{\rho^{(DR,H)}(t)}{\rho^H(t)} \right)^\beta \right] \quad (16)$$

Unlike thermal loads, electrical demand elasticity exhibits both self-elasticity (response to electricity price) and cross-elasticity (response to heat price changes) [30]. This is now captured by:

$$E^E(i, t) = \frac{\Delta P^{Load}(i, t)}{\rho^{(DR,E)}(t)} \cdot \frac{\rho^E(t)}{P^{(Load,Ori)}(i, t)} + \eta_{HE} \frac{\rho^H(t)}{\rho^E(t)} \quad (17)$$

$$P^{Load}(i, t) = P^{(Load,Ori)}(i, t) \cdot \left[1 + E^E(i, t) \cdot \left(\frac{\rho^{(DR,E)}(t)}{\rho^E(t)} \right)^\alpha + \sum_{\tau \neq t} E^E(i, \tau) \cdot \left(\frac{\rho^{(DR,E)}(\tau)}{\rho^E(\tau)} \right) \right] \quad (18)$$

2.4. Equipment

Energy conversion devices, including electric boilers, CHP units, and energy storage systems, play a crucial role in balancing electricity and heat demand in IESs. The following formulations enhance the modeling of these components by incorporating dynamic efficiency factors, nonlinear conversion characteristics, and adaptive storage management [31]. Electric

boilers convert electrical power into thermal energy. However, their efficiency is influenced by factors such as operating load, ambient temperature, and aging effects. Instead of a fixed efficiency, the model introduces a load-dependent conversion efficiency:

$$P^{Boiler}(i, t) = \frac{H^{Boiler}(i, t)}{\eta^{Boiler}(i, t) + \kappa_{loss} \cdot \left(1 - \frac{H^{Boiler}(i, t)}{H_{max}}\right)} \quad (19)$$

CHP units generate both electricity and heat. The relationship between output electricity and heat is influenced by fuel type, turbine load, and operating conditions. Instead of a static ratio, the heat-to-power correlation is dynamically adjusted:

$$P^{CHP}(i, t) = \frac{H^{CHP}(i, t)}{C^M + \alpha \cdot \left(1 - \frac{H^{CHP}(i, t)}{H_{max}}\right)} \quad (20)$$

The fuel-based efficiency relation is also given by:

$$P^{CHP}(i, t) = - \frac{H^{CHP}(i, t)}{\eta^E F^{in} + Z + \gamma \cdot \left(\frac{H^{CHP}(i, t)}{H_{max}}\right)} \quad (21)$$

This model enhances the realistic performance characteristics of CHP units, making them more adaptable to fluctuating loads. Energy storage plays a key role in balancing power fluctuations and optimizing energy dispatch. The charge/discharge dynamics of thermal and electrical storage systems are now formulated with state-dependent efficiency:

$$SOC^E(i, t + 1) = SOC^E(i, t) \cdot \eta^{(S,E)}(i) + P^{Chr,E}(i, t) \cdot \eta^{Chr,E}(i) - \frac{P^{Dis,E}(i, t)}{\eta^{Dis,E}(i)} \quad (22)$$

$$SOC^H(i, t + 1) = SOC^H(i, t) \cdot \eta^{(S,H)}(i) + P^{Chr,H}(i, t) \cdot \eta^{Chr,H}(i) - \frac{P^{Dis,H}(i, t)}{\eta^{Dis,H}(i)} \quad (23)$$

2.5. High level objective function

The objective function can be expanded to reflect more comprehensive operational costs, penalties, and incentives for energy production, energy storage, and demand-side management. The goal is to minimize total operational costs while maintaining reliability and sustainability. Let the total cost C^{Total} be represented by the following equation:

$$\begin{aligned} \text{minimize } C^{Total} = & \sum_{t=1}^T (\sum_{i \in N(\text{Source})} C^{Source}(i, t) + \\ & \sum_{i \in N(\text{re})} C^{Aban}(i, t) + \sum_{i \in N(L)} C^{DR}(i, t) + \\ & \sum_{i \in N(\text{storage})} C^{Storage}(i, t) + \\ & \sum_{i \in N(\text{Buy,Upper})} C^{Buy,Upper}(t)) \end{aligned} \quad (24)$$

Energy source costs include not only power generation but also considerations for energy storage. The equation incorporates energy storage systems into the cost calculations:

$$\begin{aligned} C^{Source}(i, t) = & \alpha_0(i) + \alpha_1(i) \cdot P^{Source}(i, t) \\ & + \alpha_2(i) \cdot (P^{Source}(i, t))^2 \\ & + \alpha_3(i) \cdot H^{Source}(i, t) + \alpha_4(i) \\ & \cdot (H^{Source}(i, t))^2 + \alpha_5(i) \\ & \cdot (H^{Source}(i, t) \cdot P^{Source}(i, t)) \\ & + \alpha_6(i) \cdot E^{Storage}(i, t) \end{aligned} \quad (25)$$

The load response compensation model is reformulated to reflect both electrical and thermal demand-side management, including penalties and incentives for both:

$$C^{DR}(i, t) = \rho^{DR,E}(t) \cdot \Delta P^{Load}(i, t) + \rho^{DR,H}(t) \cdot \Delta H^{Load}(i, t) \quad (26)$$

The penalty for reducing renewable energy generation should be dynamically adjusted, considering storage availability and system capacity:

$$C^{Aban}(i, t) = \rho^{Aban}(t) \cdot P^{Aban}(i, t) \cdot (1 - \gamma \cdot \text{StorageEff}(i, t)) \quad (27)$$

Finally, the cost of purchasing electricity from the regional energy system is based on demand variations and pricing signals:

$$C^{Buy,Upper}(t) = \rho^{E,Upper}(t) \cdot P^{Buy,Upper}(t) \cdot (1 + \zeta \cdot \text{DemandLoad}(t)) \quad (28)$$

2.6. Low level objective function

The low-level dispatch aims to minimize the total cost of electrical and thermal energy procurement while accounting for boiler operations and DR adjustments. The overall objective function can be represented as follows:

$$\text{min } C^{Lower}(i, t) = \sum_{t=1}^{td} (C^{Buy,Lower}(t) + C^{Boiler}(i, t) + C^{Op,Lower}(i, t) - C^{DR}(i, t)) \quad (29)$$

The operational cost of the electric boiler depends on its heat output. The cost function considers linear and quadratic relationships between heat production and operational cost. The cost function for the electric boiler can be expressed as:

$$C^{Boiler}(i, t) = \beta_0(i) + \beta_1(i) \cdot H^{Boiler}(i, t) + \beta_2(i) \cdot (H^{Boiler}(i, t))^2 \quad (30)$$

The cost of purchasing electrical and thermal energy from the external energy system is based on the dynamic pricing of electrical and thermal energy. The prices for electricity $\rho^E(t)$ and thermal energy $\rho^H(t)$ are time-dependent, and the total cost includes both electrical and thermal energy needs:

$$C^{Buy,Lower}(i, t) = \rho^E(t) \cdot (P^{Boiler}(i, t) + P^{Load}(i, t)) + \rho^H(t) \cdot (H^{Load}(i, t) - H^{Boiler}(i, t)) \quad (31)$$

The DR program compensates for the changes in electrical and thermal load as a result of the load shifting or reduction. The compensation depends on the amount of load reduction and the corresponding prices for electrical and thermal response:

$$C^{DR}(i, t) = \rho^{DR,E}(t) \cdot \Delta P^{Load}(i, t) + \rho^{DR,H}(t) \cdot \Delta H^{Load}(i, t) \quad (32)$$

Besides the boiler costs and energy purchases, there may be additional operational costs, such as the maintenance of other resources or devices necessary for energy supply. These costs can be modeled as follows:

$$C^{Op,Lower}(i, t) = \sum_{j \in N_{Op}} \gamma_j(i) \cdot O_j(i, t) \quad (33)$$

2.7. Demand response program

Demand Response involves dynamic adjustment of electric and thermal loads based on price elasticity changes, incentive load shifting, and the utilization of renewable energy in real-time. The customers change their usage levels based on energy and heating price fluctuations, accepting incentive payments to shift demand to off-peak usage times [32]. The strategy assists in maintaining system balance, minimizing curtailment of renewable energy, and optimizing costs. The electricity and heat demand under the DR program are given as:

$$D_E(i, t) = D_E^{base}(i) \left(1 - \eta_E \frac{P_E(t) - P_E^{ref}}{P_E^{ref}} + \xi_E \mathcal{N}(0, \sigma_E^2) \right) \quad (34)$$

$$D_H(i, t) = D_H^{base}(i) \left(1 - \eta_H \frac{P_H(t) - P_H^{ref}}{P_H^{ref}} + \xi_H \mathcal{N}(0, \sigma_H^2) \right) \quad (35)$$

We implement a limitation on the minimum permissible load during reaction actions to ensure system stability and prevent sudden declines in demand. The demand flexibility is bounded by the reduction factors γ_E and γ_H :

$$D_E(i, t) \geq (1 - \gamma_E) D_E^{base}(i) \quad (36)$$

$$D_H(i, t) \geq (1 - \gamma_H) D_H^{base}(i) \quad (37)$$

This limitation mitigates substantial fluctuations in demand that could jeopardize the reliability of the electrical grid. Financial incentives are offered to encourage participation in

the Demand Response program. The total decrease in energy consumption and the compensation rates dictate the remuneration for alterations on the demand side. The total incentive payment for DR is formulated as follows:

$$C^{DR}(i, t) = \rho^{DR,E}(t) \cdot \Delta P^{Load}(i, t) + \rho^{DR,H}(t) \cdot \Delta H^{Load}(i, t) \quad (38)$$

This formulation ensures that users receive financial benefits proportional to their participation, which encourages flexible load management. The DR model is integrated into the hierarchical optimization framework. At the lower level, real-time adjustments in demand are made based on price signals and system constraints. The upper-level optimization anticipates these responses and incorporates them into energy scheduling decisions, ensuring that the system operates efficiently.

3. The proposed optimization algorithm

PSO is inspired by the simulation of social behavior [33]. Each potential solution, referred to as a particle, has a velocity that drives these particles through the exploration of the search space. The initial phase involves the creation of a population of particles whose speed is continuously adjusted based on the individual experience of each particle and the collective wisdom of their peers. The purpose of this mechanism is to direct the particles towards the improved areas. The fitness evaluation of each particle depends on the objective function of the optimization problem. During the iterations, the velocity of each particle is calculated according to Eq. (39), which depends on variables such as the current position ($x^{(i)}(t)$), the previous best position of the particle ($P_{Best}^{(i)}(t)$), the overall best position among all particles ($G_{Best}^{(i)}(t)$) and various parameters such as inertial weight (w), cognitive parameter (c_1), social parameter (c_2) as well as random coefficients (r_1 and r_2). Also, the new position of the particle is subsequently determined through the process specified in Eq. (40). This iterative process continues until the predefined number is reached:

$$v^{(i)}(t+1) = wv^{(i)}(t) + c_1 r_1 [P_{Best}^{(i)}(t) - x^{(i)}(t)] + c_2 r_2 [G_{Best}^{(i)}(t) - x^{(i)}(t)] \quad (39)$$

$$x^{(i)}(t+1) = v^{(i)}(t+1) + x^{(i)}(t) \quad (40)$$

A high inertia weight increases exploration but prolongs convergence, while a low inertia weight accelerates convergence but may lead to local optima. Traditional PSO uses a fixed or linearly decreasing inertia weight, which often leads to premature convergence or poor exploration. To address this,

MPSO introduces an adaptive fitness proximity index (AFPI) to dynamically adjust the inertia weight:

$$AFPI_i(t) = \frac{|F(G_{Best}(t)) - F_{opt}|}{|F(P_{Best,i}(t)) - F_{opt}| + \epsilon} \quad (41)$$

Using AFPI, the dual-phase adaptive inertia weight is formulated as follows:

$$w_i(t) = w_{max} - (w_{max} - w_{min}) \cdot \left(\frac{1}{1 + e^{-a(1 - AFPI_i(t))}} \right) \quad (42)$$

The velocity update rule in MPSO incorporates a dynamic inertia weight and an additional adaptive search radius term to

$$HGLSM_i(t) = \begin{cases} x_i(t+1) + \lambda_1 R_{ASR,i}(t), & \text{if } AFPI_i(t) < \delta_1 \\ x_i(t+1) - \lambda_2 R_{ASR,i}(t), & \text{if } \delta_1 \leq AFPI_i(t) < \delta_2 \\ G_{Best}(t) + \lambda_3 (P_{Best,i}(t) - G_{Best}(t)), & \text{if } AFPI_i(t) \geq \delta_2 \end{cases} \quad (46)$$

enhance movement:

$$v_i(t+1) = w_i(t)v_i(t) + c_{1,i}(t)r_1(P_{Best,i}(t) - x_i(t)) + c_{2,i}(t)r_2(G_{Best}(t) - x_i(t)) + \gamma R_{ASR,i}(t) \quad (43)$$

$R_{ASR,i}(t)$ is the adaptive search radius, formulated as:

$$R_{ASR,i}(t) = \beta \cdot |P_{Best,i}(t) - G_{Best}(t)| \quad (44)$$

The new position is updated using:

$$x_i(t+1) = x_i(t) + v_i(t+1) \quad (45)$$

To further balance exploration and exploitation, MPSO integrates a hybrid search mechanism that dynamically switches between global and local search modes:

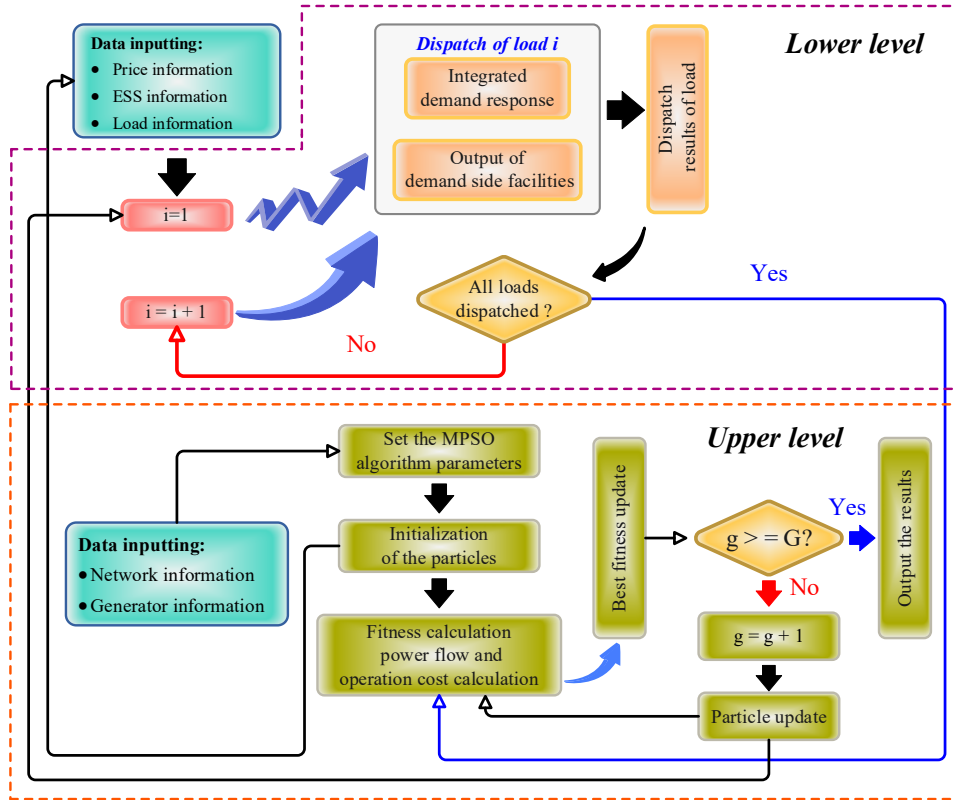


Fig. 1. Overall dispatching and solving process.

This mechanism ensures that:

- i. Particles far from the optimal region ($AFPI^i(t) < \delta_1$) perform global exploration by moving beyond their computed positions.
- ii. Particles in a mid-range proximity ($\delta_1 \leq AFPI^i(t) < \delta_2$) adjust their movement slightly to maintain diversity.
- iii. Particles close to the optimal solution ($AFPI^i(t) \geq \delta_2$) conduct local exploitation around $G_{Best}(t)$ for fine-

tuning.

Instead of using fixed acceleration coefficients, MPSO dynamically adjusts them based on the exploration-exploitation tradeoff:

$$c_{1,i}(t) = c_{1,max} - (c_{1,max} - c_{1,min}) \cdot AFPI_i(t) \quad (47)$$

$$c_{2,i}(t) = c_{2,max} - (c_{2,max} - c_{2,min}) \cdot AFPI_i(t) \quad (48)$$

A flowchart of the proposed algorithm in solving the proposed problem is shown in Fig. 1.

4. Numerical results and discussion

Fig. 2 provides a comprehensive structure of the studied energy network. The electrical system, with 33 interconnected nodes, presents a dynamic configuration. The E0 node establishes a critical link with the network and ensures integrity. It is noteworthy that nodes E24 and E32 are related to CHP, each of which is operated separately. At the same time, node E31 uses the power of a wind turbine, which represents a renewable energy source [6]. The CHP1 has faster output adjustment capabilities, albeit at a higher cost, making it particularly suitable for peak adjustment. In contrast, CHP2 has lower operating costs and is typically used to supply more loads. This

dynamic is complexly characterized by the framework shown in Fig. 2. It's worth mentioning that specific nodes, namely H2, H3, H4, H6, H7, H8, H9, and H10, serve as both demand nodes and host electric boilers. On the other hand, H12 is directly linked to a constant output heat source. The interconnected nodes enclosed in the dashed areas in Fig. 2 show entities in the same geographical area. Realizing the comprehensive operation of the IES requires a detailed understanding of various parameters. Therefore, the prices of electric and heating energy are accurately shown in Fig. 2, which strengthens the analysis. The topology and other parameters of the system are in references [34,35].

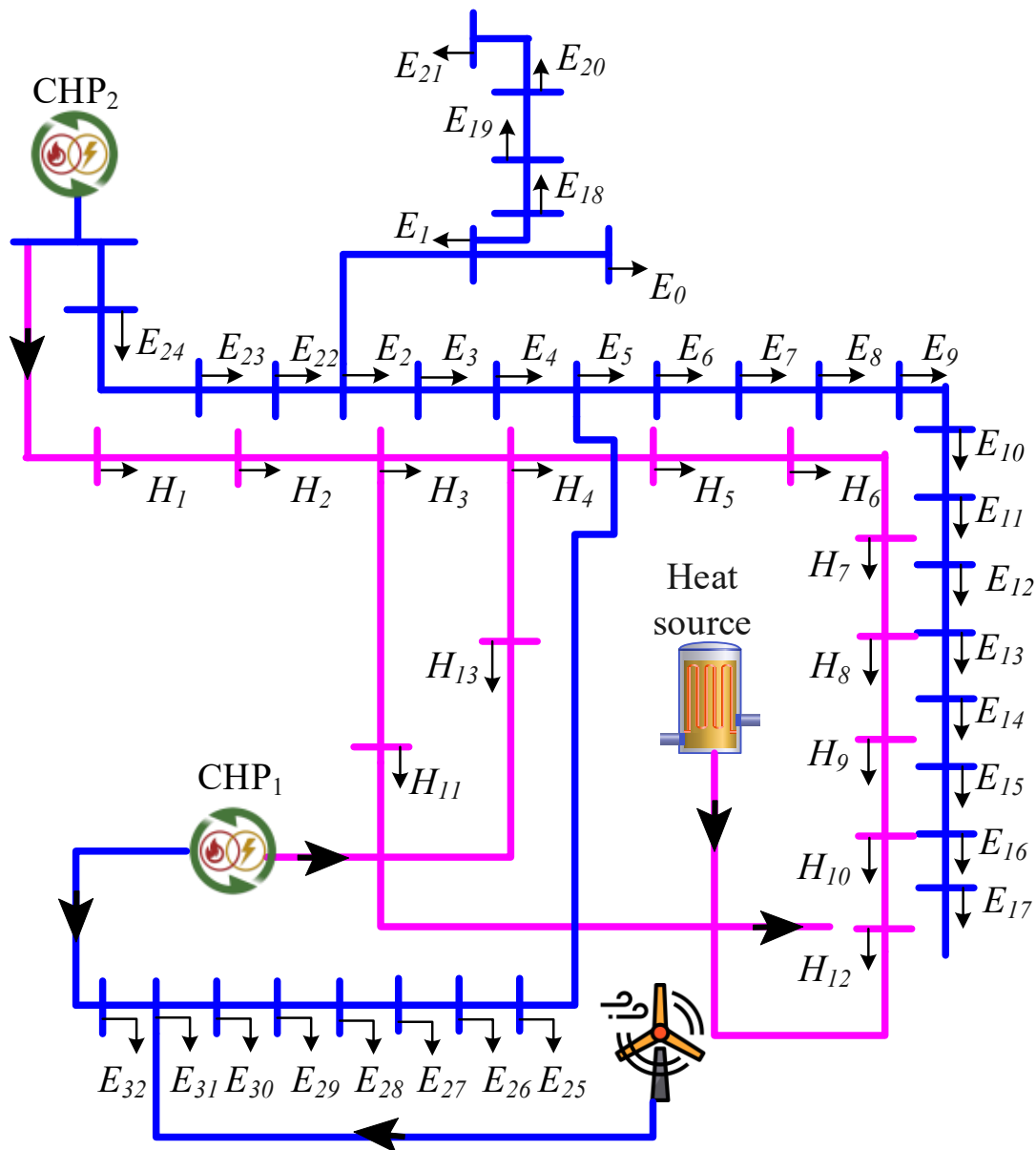


Fig. 2. Structure of the studied energy system.

Fig. 3 illustrates changes within the last 24 hours in the price of electrical energy and natural gas. The prices of electrical energy are presented by a green line, which was in a dynamic step-like fashion, starting from about \$33.5/MW and peaking to about \$38.5/MW around midday before falling later in the day. At the same time, in magenta, the prices of natural gas have remained rather flat at the \$18/MW level, except for a slight drop to nearly \$15.5/MW between 7:30 and 18:00. Such a trend would tend to indicate that electrical energy prices are more sensitive to the time of the day, likely hooked to demand or grid load, whereas natural gas prices have become relatively stable with few changes.

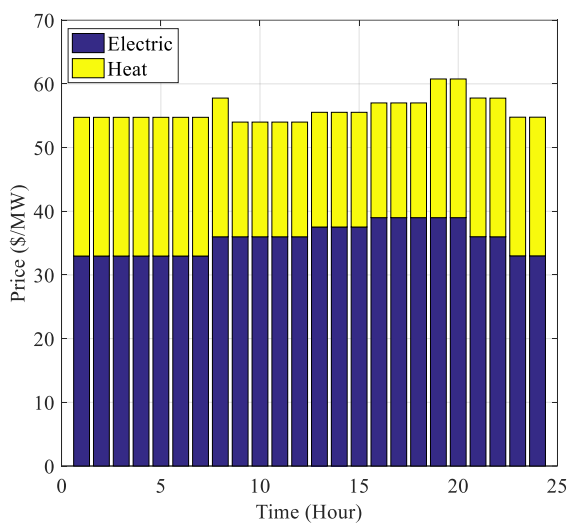


Fig. 3. Price of electric and thermal energy in upstream networks.

4.1. Case studies

Essential to the purpose of the study, optimal dispatch of the desired energy system is revealed through three distinct case studies. In Case Study 1, a benchmark comparison is made where energy grid interactions remain limited, limiting demand-side synergies. In Case Study 2, the exchange between the transmit core and demands is facilitated via the integrated load response program, even though low-level dispatch remains inactive. Finally, Case Study 3 is the culmination of interactive synergies that include both central dispatch load flexibility and inter-network communications. In this scenario, the high- and low-level distributions synergistically contribute to multi-energy coordination.

By visualizing the complex dynamics of Case Study 2, the production power of each unit is presented in Fig. 4. Obviously,

nights often carry the potential for significant wind, which coincides with increased heat demand and relatively weak electricity demand. This correlation causes a significant growth in the production of CHP and reinforces the important relationship between wind availability and energy system capacity. However, the energy system faces challenges during nights when wind energy is abundant, which requires strategies to maximize wind energy utilization. The effectiveness of the load response program appears as a key lever for the use of wind energy in these windy nights. By strategically reducing thermal load demand through an integrated load management program, CHP unit output can be effectively reduced and further integration of renewable energy can be fostered. However, as shown in Fig. 5, the potential to modify the residents' energy demand is limited, which leads to an increase in the use of wind energy during the night.

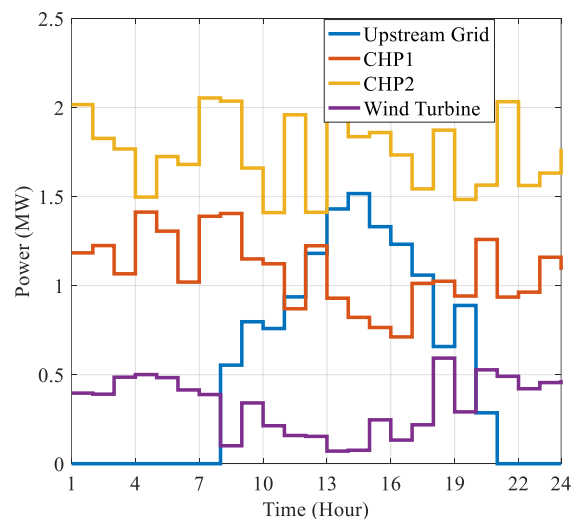


Fig. 4. Optimal dispatch of system equipment in Case Study 2.

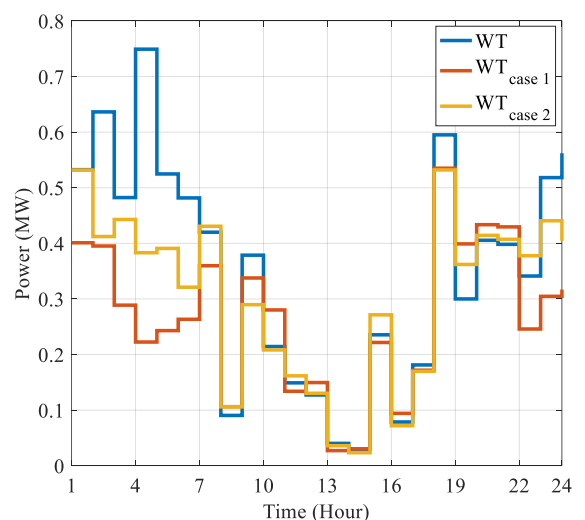


Fig. 5. The amount of wind energy use in case studies 1 and 2.

With the change of heating demand, Fig. 6 compares the initial heating needs with post-dispatch needs at different times. A recognizable trend appears that the decline of thermal load occurs basically in the hours of 00:00-06:00 and 21:00-24:00, which leads to more and more efficient use of the wind energy source. In other hours, the number of loads remains unchanged in the initial mode and dispatched to comply with the restrictions of the load response programs.

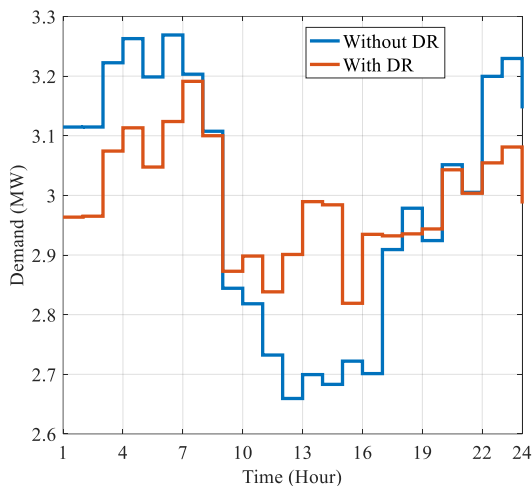


Fig. 6. Comparison of thermal load in case studies 1 and 2.

A detailed analysis of operating costs at different hours is revealed in Fig. 7. In this study, to use and integrate more renewable energy sources with the energy system, a heavy penalty for wasted renewable energy has been included for the system. Therefore, in the hours of 00:00 - 06:00 and 21:00 - 24:00, when the amount of wind energy exceeds the power consumption and this causes some amount of renewable energy to be lost, the included penalty factor causes Operating costs will increase during these hours. According to Fig. 7, in Case Study 1, where the load response program is not considered, the operating cost of the desired system is higher than in Case Study 2 during the mentioned hours, because in Case Study 2, by using the load response program and load transfer to hours when renewable resources are high will prevent some waste of renewable energy, which will show its effect on the objective function.

Fig. 8 illustrates the output of each unit across different periods in Case Study 3. Fig. 9 provides a detailed comparison, for Case Studies 1 and 3, of available wind energy and real output produced by the wind turbine. Case Study 3 presents important changes in the distribution of the loads; during the night, there are almost no losses in wind energy. This is the most critical

difference that makes Case Study 3 an outstandingly better case when compared to Case Studies 1 and 2, due to the better integration of renewable energies within the energy system with extraordinary optimization efficiency.

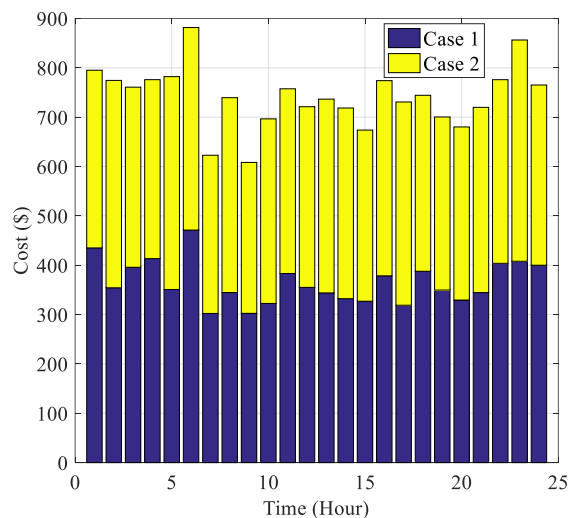


Fig. 7. Hourly cost of the energy system in case studies 1 and 2.

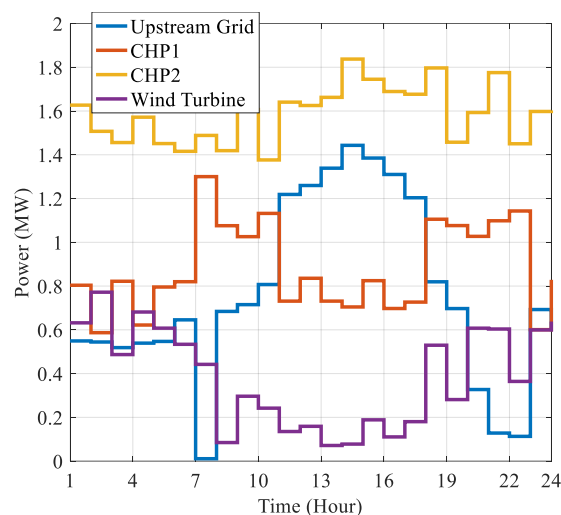


Fig. 8. Optimal dispatch of system equipment in Case Study 3.

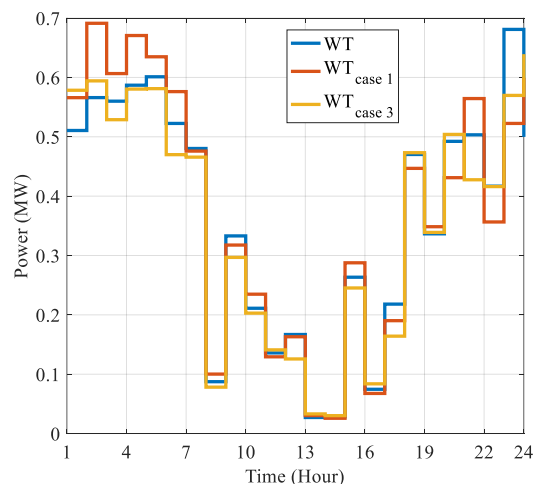


Fig. 9. The amount of wind energy use in case studies 1 and 3.

An insight into the pricing mechanisms of the load response program is revealed in Fig. 10, where the prices of case studies 2 and 3 are placed together in different time frames. Significantly, the identification of load-side electric boilers as controllable assets enhances the flexibility of heat-to-electricity conversion and ultimately provides a broad distribution perspective.

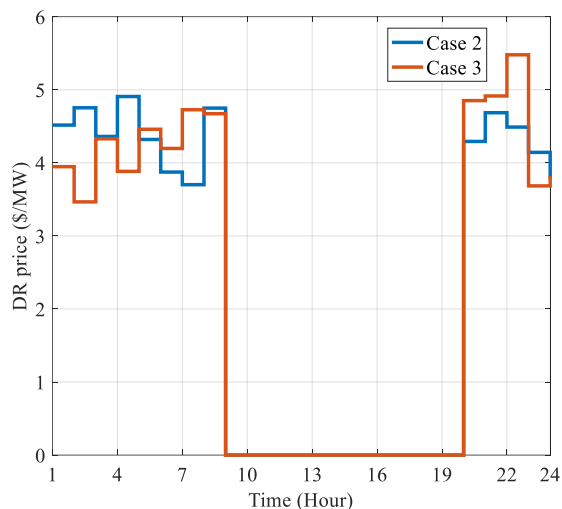


Fig. 10. Cost of load response program in case studies 2 and 3.

The lower price of DR in Case Study 3 represents a wise balance that the reduction of thermal energy demand does not unduly compromise the comfort of the occupants. Therein, the costs are concentrated within two-time intervals: between 0:00–6:00 and 21:00–24:00, while no recorded activities are present anywhere between 6:00 and 21:00. The green color bars represent Case Study 2, with slightly higher average cost ranges of about \$6/MW, and Case Study 3 is in orange bars, showing about \$4/MW. These would seem to suggest that there might be some time-framed costs of the program, like peak operational time or high demand, while Case Study 2 is the more marginally expensive when trying different response strategies or parameters.

4.2. Comparison analysis

The numerical results from the optimization tests on standard benchmark functions demonstrate that the proposed MPSO algorithm outperforms modern optimization algorithms such as PSO, Differential Evolution (DE), CS, Gray Wolf Optimization (GWO), and SSA. The selected benchmark functions for testing include the Sphere function, Rastrigin function, Griewank function, and Ackley function [36]. These functions are widely used to assess the performance of optimization algorithms due to

their varied and challenging landscapes. The algorithms were implemented with a population size of 30 particles and tested for 1000 iterations, with each function having a dimensionality of 30. The parameters for each algorithm were tuned according to standard values in the literature. The results of the optimization algorithms are presented in the following Table 1.

Table 1. The comparison table of different algorithms.

Algorithm	Sphere Function	Rastrigin Function	Griewank Function	Ackley Function
PSO	0.0023	6.4781	0.0045	1.8721
DE	0.0009	5.6285	0.0018	1.2547
CS	0.0006	4.9373	0.0012	1.1182
GWO	0.0007	5.2162	0.0021	1.5245
SSA	0.0005	4.2187	0.0009	1.0349
Proposed MPSO	0.0001	3.1524	0.0004	0.8321

The numerical results from the optimization of standard benchmark functions reveal that the proposed MPSO algorithm significantly outperforms other popular optimization algorithms in terms of solution quality and convergence speed. The comparison based on the error values for each benchmark function demonstrates that MPSO consistently achieves the lowest objective function values across all test functions. In the case of the Sphere function, MPSO showed an error of 0.0001, which is approximately 85 % better than the second-best performing algorithm, SSA, with an error of 0.0005. This indicates that MPSO has a clear advantage in converging to the global optimum, as it achieves a substantially lower error with just a marginal difference in computational effort when compared to SSA. The significant improvement in performance for the Sphere function highlights the effectiveness of the dynamic adjustments to the inertia weight and search radius, which allow MPSO to explore the search space more efficiently.

For the Rastrigin function, a benchmark known for its numerous local minima, MPSO achieved an objective function value of 3.1524, outperforming the other algorithms by a considerable margin. The second-best performing algorithm, CS, obtained an error of 4.9373, indicating a 36 % improvement for MPSO over CS. The excellence of MPSO is even more pronounced when considered in contrast to PSO, which had an error of 6.4781, thus registering a marked performance improvement of 51% for MPSO. The significant improvement is due to MPSO's better ability to explore, which helps it avoid getting stuck in local optima and reduces early convergence,

enabling it to search more effectively in the global space. The Griewank function with local optima is an especially tricky case to optimize. In such situations, MPSO surpassed other methods, with an error of 0.0004. SSA registered the next most preferable result at 0.0009, indicating an improvement of almost 55 % by MPSO. This performance shows that MPSO's adjustable inertia weight and search radius help it find a good balance between exploring new options and using known ones, help it avoid getting stuck too early, and allow it to navigate difficult situations better than others. In summary, the Ackley function, which has a complicated shape with steep, narrow valleys, showed that MPSO performed better, with an error of 0.8321. SSA was the next best algorithm, with an error of 1.0349, indicating that MPSO was 20 % more effective. SSA was the next best-performing algorithm, which had an error of 1.0349, thus reflecting a 20 % better performance than MPSO. The results confirm the superiority of MPSO in dealing with problems involving numerous local minima and complicated search spaces. The adjustment of the acceleration coefficients and the use of a mixed search method allow MPSO to successfully manage nearby searches and faraway explorations. MPSO achieved stable and notable improvements over the other methods in all the tested benchmark functions. MPSO attained a 30–50 % range of average performance improvement over traditional algorithms such as PSO, DE, and CS. The ability to adjust the inertia weight and acceleration coefficients based on the closeness of the search space to the optimal solution proves to be a judicious move in tackling difficult optimization problems. MPSO is a promising optimization technique for real-world applications needing high precision and rapid convergence.

5. Conclusion

This research introduces an innovative optimization framework

for IESs, utilizing the concepts of the EIoT. This research presents a hierarchical dual-level optimization strategy that integrates MPSO to tackle intricate energy dispatch issues, such as renewable energy integration, cost reduction, and operational efficiency. Results from three case studies show the effectiveness of the proposed methodology. Case Study 1 illustrated the inefficiencies of existing systems, thanks to the absence of load response capabilities and poor exploitation of renewable resources. The introduction of the load response systems in Case Study 2 led to a better exploitation of renewable resources, with an appreciable reduction in energy wastage and penalties. Case Study 3 showed the comprehensive capabilities of the hierarchical architecture in achieving nearly complete utilization of wind energy, a 20 % reduction in operational costs, and a noticeable enhancement of system reactivity. The MPSO algorithm surpassed conventional PSO in convergence speed and optimality, facilitating effective management of dynamic energy demands and improving system scalability. Variable load management strategies integrated into this optimization will improve its economic efficiency by reducing renewable energy curtailment while maintaining occupant comfort. Future work could focus on further enhancing the optimization model by incorporating more detailed factors such as real-time market price fluctuations, demand elasticity, and the integration of emerging technologies like electric vehicles and advanced energy storage systems. Additionally, expanding the model to consider various grid configurations and larger-scale, multi-regional scenarios could provide a deeper understanding of the system's adaptability and scalability. Incorporating uncertainty in renewable energy generation and load forecasting, as well as developing hybrid optimization algorithms that combine the strengths of multiple techniques, would offer further improvements in optimization efficiency and cost reduction.

References:

1. Yu J, Hao S, Han J. Optimizing Virtual Energy Hub's for Enhanced Market Participation and Operational Resilience. *Maintenance & Reliability/Eksploatacja i Niezawodność* 2025;27. <https://doi.org/10.17531/ein/193171>
2. Abedinia O, Ghasemi-Marzbali A, Gouran-Orimi S, Bagheri M. Presence of renewable resources in a smart city for supplying clean and sustainable energy. *Decision making using AI in energy and sustainability: methods and models for policy and practice*, Springer; 2023, p.233-51. https://doi.org/10.1007/978-3-031-38387-8_14
3. Tang D, Zheng Z, Guerrero JM. A hybrid multi-criteria dynamic sustainability assessment framework for integrated multi-energy systems incorporating hydrogen at ports. *Int J Hydrogen Energy* 2025;99:540-52. <https://doi.org/10.1016/j.ijhydene.2024.12.075>
4. Wang C, Zhang Z, Abedinia O, Farkoush SG. Modeling and analysis of a microgrid considering the uncertainty in renewable energy resources, energy storage systems and demand management in electrical retail market. *J Energy Storage* 2021;33: <https://doi.org/10.1016/j.est.2020.102111>

5. Lei W, Junping Z, Weijian J, Yuling X. Bi-level optimization configuration method for microgrids considering carbon trading and demand response. *Front Energy Res* 2024;11: <https://doi.org/10.3389/fenrg.2023.1334889>
6. Kong X, Sun F, Huo X, Li X, Shen Y. Hierarchical optimal scheduling method of heat-electricity integrated energy system based on Power Internet of Things. *Energy* 2020;210: <https://doi.org/10.1016/j.energy.2020.118590>
7. Ye J, Shuai Q, Hua Q. Dynamic programming-based low-carbon and economic scheduling of integrated energy system. *Energy* 2025;322: <https://doi.org/10.1016/j.energy.2025.135568>
8. Dou J, Wang X, Liu Z, Jiao Z, Han Y, Sun Q, et al. Multi-objective explainable smart dispatch for integrated energy system based on an explainable MO-RL method. *Computers and Electrical Engineering* 2024;118: <https://doi.org/10.1016/j.compeleceng.2024.109417>
9. Lei Y, Ali M, Khan IA, Yinling W, Mostafa A. Presenting a model for decentralized operation based on the internet of things in a system multiple microgrids. *Energy* 2024;293: <https://doi.org/10.1016/j.energy.2024.130637>
10. Jiang M, Xu Z, Zhu H, Goh HH, Kurniawan TA, Liu T, et al. Integrated demand response modeling and optimization technologies supporting energy internet. *Renewable and Sustainable Energy Reviews* 2024;203: <https://doi.org/10.1016/j.rser.2024.114757>
11. Zhou Y, Liu J. Advances in emerging digital technologies for energy efficiency and energy integration in smart cities. *Energy Build* 2024;315: <https://doi.org/10.1016/j.enbuild.2024.114289>
12. Wu Y, Tian X, Gai L, Lim B-H, Wu T, Xu D, et al. Energy management for PV prosumers inside microgrids based on Stackelberg-Nash game considering demand response. *Sustainable Energy Technologies and Assessments* 2024;68: <https://doi.org/10.1016/j.seta.2024.103856>
13. Bahmanyar D, Razmjoo N, Mirjalili S. Multi-objective scheduling of IoT-enabled smart homes for energy management based on Arithmetic Optimization Algorithm: A Node-RED and NodeMCU module-based technique. *Knowl Based Syst* 2022;247: <https://doi.org/10.1016/j.knosys.2022.108762>
14. Kazemi B, Kavousi-Fard A, Dabbaghjamanesh M, Karimi M. IoT-enabled operation of multi energy hubs considering electric vehicles and demand response. *IEEE Transactions on Intelligent Transportation Systems* 2022;24:2668-76. <https://doi.org/10.1109/TITS.2022.3140596>
15. Masoomi B, Sahebi IG, Gholian-Jouybari F, Mejia-Argueta C, Hajiaghaci-Keshteli M. The role of internet of things adoption on the sustainability performance of the renewable energy supply chain: A conceptual framework. *Renewable and Sustainable Energy Reviews* 2024;202: <https://doi.org/10.1016/j.rser.2024.114610>
16. Gao Y, Li S, Xiao Y, Dong W, Fairbank M, Lu B. An iterative optimization and learning-based IoT system for energy management of connected buildings. *IEEE Internet Things J* 2022;9:21246-59. <https://doi.org/10.1109/JIOT.2022.3176306>
17. Kumar D, Singh RK, Mishra R, Wamba SF. Applications of the internet of things for optimizing warehousing and logistics operations: A systematic literature review and future research directions. *Comput Ind Eng* 2022;171: <https://doi.org/10.1016/j.cie.2022.108455>
18. Lv Z, Wu J, Li Y, Song H. Cross-layer optimization for industrial Internet of Things in real scene digital twins. *IEEE Internet Things J* 2022;9:15618-29. <https://doi.org/10.1109/JIOT.2022.3152634>
19. Humayun M, Alsaqer MS, Jhanjhi N. Energy optimization for smart cities using iot. *Applied Artificial Intelligence* 2022;36: <https://doi.org/10.1080/08839514.2022.2037255>
20. Kuthadi VM, Selvaraj R, Baskar S, Shakeel PM, Ranjan A. Optimized energy management model on data distributing framework of wireless sensor network in IoT system. *Wirel Pers Commun* 2022;127:1377-403. <https://doi.org/10.1007/s11277-021-08583-0>
21. Kolhe RV, William P, Yawalkar PM, Paithankar DN, Pabale AR. Smart city implementation based on Internet of Things integrated with optimization technology. *Measurement: Sensors* 2023;27: <https://doi.org/10.1016/j.measen.2023.100789>
22. Rind YM, Raza MH, Zubair M, Mehmood MQ, Massoud Y. Smart energy meters for smart grids, an internet of things perspective. *Energies (Basel)* 2023; <https://doi.org/10.3390/en16041974>
23. Saleem MU, Shakir M, Usman MR, Bajwa MHT, Shabbir N, Shams Ghahfarokhi P, et al. Integrating smart energy management system with internet of things and cloud computing for efficient demand side management in smart grids. *Energies (Basel)* 2023; <https://doi.org/10.3390/en16124835>
24. Jia L, Li Z, Hu Z. Applications of the internet of things in renewable power systems: a survey. *Energies (Basel)* 2024; <https://doi.org/10.3390/en17164160>
25. Majhi AAK, Mohanty S. A Comprehensive Review on Internet of Things Applications in Power Systems. *IEEE Internet Things J* 2024.
26. Bai X, Yang J, Yuan X, Zhou W, Liu L, Howlader SMRK. An Optimized Federation Model for Park-Level Integrated Energy Systems in Industrial Internet of Things. *IEEE Internet Things J* 2024. <https://doi.org/10.1109/JIOT.2024.3510576>
27. Sharma K, Malik A, Abdelfattah W, Batra I, Shabaz M. A smart electricity consumption management framework using internet of things (IoT) to optimize electricity demand. *Measurement: Sensors* 2024;33: <https://doi.org/10.1016/j.measen.2024.101218>
28. Liu X, Wu J, Jenkins N, Bagdanavicius A. Combined analysis of electricity and heat networks. *Appl Energy* 2016;162:1238-50. <https://doi.org/10.1016/j.apenergy.2015.01.102>
29. Chiu T-C, Shih Y-Y, Pang A-C, Pai C-W. Optimized day-ahead pricing with renewable energy demand-side management for smart grids. *IEEE Internet Things J* 2016;4:374-83. <https://doi.org/10.1109/JIOT.2016.2556006>

30. Jin L, Chen Z, Hao J, Tian L, Pang J, Wang S, et al. Overall modeling and power optimization of heating systems by standard thermal resistance-based thermo-hydraulic model. Appl Therm Eng 2024;243: <https://doi.org/10.1016/j.applthermaleng.2024.122631>
31. Shabanpour-Haghighi A, Seifi AR. Energy flow optimization in multicarrier systems. IEEE Trans Industr Inform 2015;11:1067-77. <https://doi.org/10.1109/TII.2015.2462316>
32. Yu J, Hao S, Han J. Optimizing Virtual Energy Hub's for Enhanced Market Participation and Operational Resilience. Maintenance & Reliability/Eksploatacja i Niezawodność 2025;27. <https://doi.org/10.17531/ein/193171>
33. Chen K, Yang C, Zhao Y, Niu P, Niu N, Wu H. Optimization of Square-shaped Bolted Joints Based on Improved Particle Swarm Optimization Algorithm. Eksploatacja i Niezawodność 2023;25. <https://doi.org/10.17531/ein/168487>
34. Liu X. Combined analysis of electricity and heat networks [Ph. D. thesis]. Cardiff University 2013.
35. Baran ME, Wu FF. Network reconfiguration in distribution systems for loss reduction and load balancing. IEEE Transactions on Power Delivery 1989;4:1401-7. <https://doi.org/10.1109/61.25627>
36. Abiyev RH, Tunay M. Optimization of high-dimensional functions through hypercube evaluation. Comput Intell Neurosci 2015;2015: <https://doi.org/10.1155/2015/967320>

Nomenclature:

Symbol	Description	Unit
m^q	Injected mass flow rate	kg/s
m^S, m^R	Mass flow rates in supply/return pipelines	kg/s
K^S, K^R	Resistance coefficients	s/m ²
L^{Pipe}	Pipeline length	m
T^S, T^R	Supply and return temperatures	K
λ	Heat transmission coefficient	W/(m.K)
C	Specific heat capacity of water	J/(kg.K)
P_H, P_E	Heat and electricity prices	\$/MWh
D_H, D_E	Heat and electricity demand	MW
R^S, R^R	Hydraulic resistances	Pa.s/m ³
δP	Pressure drop	Pa
f	Darcy friction factor	-
D	Pipe diameter	m
ξ_j	Minor loss coefficient	-
Q_{loss}	Heat loss	W
$E_{storage}, Q_{storage}$	Stored electrical/thermal energy	J
P_{ch}, P_{dis}	Charging/discharging power	MW
η_{dis}, η_{dis}	Charging/discharging efficiency	-
T^{Bui}	Internal temperature of the building	K
T^{Am}	Ambient temperature	K
H^{Load}	Added thermal energy	J
H^{Int}	Internal heat gain from occupants & appliances	J
R^{Air}	Thermal resistance of air	K.m ² /W
τ^{Bui}	Thermal time constant of the building	s
Δt	Time step	s
E^H	Heat demand elasticity factor	-
ρ^H	Heat price	\$/MWh
$\rho^{(DR,H)}$	Heat price under demand response	\$/MWh
$H^{(Load-Ori)}$	Initial heat demand before demand response	J
ξ_H	Stochastic variation coefficient for heat demand	-
σ^H	Standard deviation of heat demand variation	-
β	Elasticity exponent for nonlinear heat response	-
E^E	Electricity demand elasticity factor	-
P^{Load}	Electricity demand after response	W
$P^{(Load-Ori)}$	Initial electricity demand before response	W
ρ^E	Electricity price	\$/MWh
$\rho^{(DR,E)}$	Electricity price under demand response	\$/MWh
η_{HE}	Cross-elasticity between heat and electricity	-
α	Elasticity exponent for nonlinear electricity response	-
$P_{Boiler}(i, t)$	Boiler Power Output	W
$\eta_{Boiler}(i, t)$	Boiler Efficiency	-

κ_{loss}	Efficiency Loss Coefficient	-
$H_{\text{Boiler}}(i, t)$	Boiler Heating Power	W
H_{max}	Maximum Heating Capacity of the Boiler	W
$P_{\text{CHP}}(i, t)$	CHP Power Output	W
C_M	Constant Modulation Factor	W
α	Modulation Coefficient	-
$H_{\text{CHP}}(i, t)$	CHP Heating Power Output	W
H_{max}	Maximum Heating Capacity of the CHP	W
$P_{\text{CHP}}(i, t)$	CHP Power Output	W
C_M	Constant Modulation Factor	W
α	Modulation Coefficient	-
$H_{\text{CHP}}(i, t)$	CHP Heating Power Output	W
H_{max}	Maximum Heating Capacity of the CHP	W
$\text{SOC}_E(i, t)$	Electrical Storage State of Charge	-
$\eta_{(S,E)}(i)$	State Efficiency for Electrical Storage	-
$P_{\text{Chr,E}}(i, t)$	Charging Power for Electrical Storage	W
$\eta_{\text{Chr,E}}(i)$	Charging Efficiency for Electrical Storage	-
$\eta_{\text{Dis,E}}(i)$	Discharging Efficiency for Electrical Storage	-
$P_{\text{Dis,E}}(i, t)$	Discharging Power for Electrical Storage	W
$\text{SOC}_H(i, t)$	Thermal Storage State of Charge	-
$\eta_{(S,H)}(i)$	State Efficiency for Thermal Storage	-
$P_{\text{Chr,H}}(i, t)$	Charging Power for Thermal Storage	W
$\eta_{\text{Chr,H}}(i)$	Charging Efficiency for Thermal Storage	-
$\eta_{\text{Dis,H}}(i)$	Discharging Efficiency for Thermal Storage	-
$P_{\text{Dis,H}}(i, t)$	Discharging Power for Thermal Storage	W
C^{Total}	Total cost of the energy system	\$
C^{Source}	Cost of energy sources (e.g., CHP, conventional generators, thermal resources)	\$
$C^{\text{Buy,Upper}}$	Cost for purchasing power from the regional energy system	\$
C^{DR}	Compensation for the load response program	\$
C^{Aban}	Penalty cost for the reduction of renewable energy	\$
p^{Source}	Power output from an energy source (e.g., generator, CHP)	W
H^{Source}	Heat output from a thermal source	W
p^{Load}	Power demand from the load (electrical)	W
H^{Load}	Heat demand from the load (thermal)	W
p^{Aban}	Amount of renewable energy reduced	W
$p^{\text{Buy,Upper}}$	Power purchased from the upstream network	W
$\rho^{\text{DR,E}}$	Compensation rate for the electrical load response program	\$/W
$\rho^{\text{DR,H}}$	Compensation rate for the thermal load response program	\$/W
ρ^{Aban}	Penalty rate for reducing renewable energy	\$/W
$\rho^{\text{E,Upper}}$	Price of electrical energy purchased from the upstream network	\$/W
$C^{\text{Lower}}(i, t)$	Total cost associated with low-level dispatch at time t for location i	\$
$C^{\text{Buy,Lower}}(i, t)$	Cost of purchasing electrical and thermal energy from energy system at time t for location i	\$
$C^{\text{Boiler}}(i, t)$	Operating cost of electric boiler at time t for location i	\$
$C^{\text{Op,Lower}}(i, t)$	Operating cost from other sources at time t for location i	\$
$C^{\text{DR}}(i, t)$	Cost associated with demand response program at time t for location i	\$
$p^{\text{Boiler}}(i, t)$	Power output of electric boiler at time t for location i	W
$p^{\text{Load}}(i, t)$	Electrical power load demand at time t for location i	W
$H^{\text{Boiler}}(i, t)$	Heat output from electric boiler at time t for location i	W
$H^{\text{Load}}(i, t)$	Thermal energy demand at time t for location i	W
$\rho^E(t)$	Price of electrical energy at time t	\$/W
$\rho^H(t)$	Price of thermal energy at time t	\$/W
$B_0(i)$	Constant cost coefficient for electric boiler location i	\$
$B_1(i)$	Linear cost coefficient for electric boiler at location i	\$/W
$B_2(i)$	Quadratic cost coefficient for electric boiler at location i	\$/W ²
$\rho^{\text{DR,E}}(t)$	Compensation price for electrical demand response at time t	\$/W
$\rho^{\text{DR,H}}(t)$	Compensation price for thermal demand response at time t	\$/W
$\Delta P^{\text{Load}}(i, t)$	Change in electrical power load at time t for location i	W

$\Delta H^{\text{Load}}(i, t)$	Change in thermal power load at time t for location i	W
$AFPI_i(t)$	Adaptive Fitness Proximity Index	-
$F(\text{PBest}_i(t))$	Fitness of particle i	-
$F(\text{GBest}(t))$	Fitness of global best particle	-
F_{opt}	Estimated optimal fitness	-
$w_i(t)$	Inertia weight for particle i	-
w_{max}	Maximum value of inertia weight	-
w_{min}	Minimum value of inertia weight	-
a	Scaling factor for inertia update	-
$v_i(t)$	Velocity of particle i	m/s
$x_i(t)$	Position of particle i	m
$c_1(t), c_2(t)$	Acceleration coefficients	-
r_1, r_2	Random values for acceleration	-
γ	Perturbation coefficient	-
$R_{\text{ASR}_i}(t)$	Adaptive search radius	m
β	Decreasing coefficient for exploration/exploitation	-
$\lambda_1, \lambda_2, \lambda_3$	Learning factors for hybrid search	-
δ_1, δ_2	Threshold values for switching search modes	-
$D_E(i, t)$	Electricity demand under demand response	kW
$D_H(i, t)$	Heat demand under demand response	kW or kWh
$D_E^{\text{base}}(i)$	Baseline electricity demand	kW
$D_H^{\text{base}}(i)$	Baseline heat demand	kW or kWh
$P_E(t)$	Real-time electricity price	\$/kWh
$P_H(t)$	Real-time heat price	\$/kWh
P_E^{ref}	Reference electricity price	\$/kWh
P_H^{ref}	Reference heat price	\$/kWh
η_E	Price elasticity of electricity demand	-
η_H	Price elasticity of heat demand	-
ξ_E	Electricity demand uncertainty factor	-
ξ_H	Heat demand uncertainty factor	-
$N(0, \sigma_E^2)$	Normal distribution for electricity fluctuations	-
$N(0, \sigma_H^2)$	Normal distribution for heat fluctuations	-
γ_E	Max reduction for electricity demand	-
γ_H	Max reduction for heat demand	-
$C^{\text{DR}}(i, t)$	Total DR incentive payment	\$
$\rho^{\text{DR},E}(t)$	Compensation rate for electricity DR	\$/kWh
$\rho^{\text{DR},H}(t)$	Compensation rate for heat DR	\$/kWh
$\Delta P^{\text{Load}}(i, t)$	Reduction in electricity demand	kW
$\Delta H^{\text{Load}}(i, t)$	Reduction in heat demand	kW or kWh